Published in final edited form as:
IEEE J Sel Top Quantum Electron. 2012 ; 18(1): 389–398.

Pulse Shaping and Evolution in Normal-Dispersion Mode-Locked Fiber Lasers

William H. Renninger, **Andy Chong**, and **Frank W. Wise**
Department of Applied Physics, Cornell University, Ithaca, NY 14853 USA

William H. Renninger: whr6@cornell.edu; Andy Chong: cyc26@cornell.edu; Frank W. Wise: fwise@ccmr.cornell.edu

Abstract

Fiber lasers mode locked with large normal group-velocity dispersion have recently achieved femtosecond pulse durations with energies and peak powers at least an order of magnitude greater than those of prior approaches. Several new mode-locking regimes have been demonstrated, including self-similar pulse propagation in passive and active fibers, dissipative solitons, and a pulse evolution that avoids wave breaking at high peak power but has not been reproduced by theoretical treatment. Here, we illustrate the main features of these new pulse-shaping mechanisms through the results of numerical simulations that agree with experimental results. We describe the features that distinguish each new mode-locking state and explain how the interplay of basic processes in the fiber produces the balance of amplitude and phase evolutions needed for stable high-energy pulses. Dissipative processes such as spectral filtering play a major role in normal-dispersion mode locking. Understanding the different mechanisms allows us to compare and contrast them, as well as to categorize them to some extent.

Index Terms

Dissipative solitons (DS); fiber lasers; self-similarity

I. Introduction

Fiber lasers offer several clear advantages over solid-state systems: compact design, thermal management, minimal alignment, spatial beam quality, and low cost. Consequently, fiber systems have become a valued option for applications requiring continuous wave or long-pulse operation. However, for pulsed operation, the benefits of fiber come at the cost of tighter confinement of the light, leading to the accumulation of nonlinear phase shifts that can rapidly degrade the pulse. For this reason, the performance of mode-locked fiber lasers has until recently lagged behind that of their solid-state counterparts. Nonetheless, recent developments in managing nonlinear phase shifts have led to mode-locked fiber systems with performance that directly competes with solid-state systems [1].

Ultrashort pulses are stabilized in an oscillator when the effects of optical nonlinearity are exactly balanced by other processes after one cycle around the cavity. The most common way to compensate nonlinearity is through group-velocity dispersion (GVD). When the GVD is anomalous, pulses are formed by a balance between positive nonlinear and negative dispersive phase changes. The resulting soliton propagates indefinitely without change. Larger phase shifts can be balanced as long as the simple relation, $E\tau \propto \beta_2/n_2$ (E is the pulse

Color versions of one or more of the figures in this paper are available online at http://ieeexplore.ieee.org.

energy, τ the pulse duration, β_2 the GVD coefficient, and n_2 the nonlinear index) holds. Before 1993, researchers operated fiber lasers almost exclusively with large net anomalous GVD, in the soliton-like regime. While the soliton-like mode-locking regime is highly robust and the pulse output is transform limited, the pulse energy (peak power) has been experimentally limited to ~0.1 nJ (<1 kW) in single-mode fiber (SMF). The limitation arises from the tendency of solitons to fission in the presence of perturbations, or from peak power clamping in an effective saturable absorber [2].

The combination of solitons and chirped pulses allows for higher pulse energies because a chirped pulse has more energy than a transform-limited pulse of equal peak power and nonlinear phase accumulation. In a laser with segments of large and nearly equal magnitudes of GVD but with opposite signs (referred to as a dispersion map), a pulse will stretch and compress and the nonlinear phase is exactly balanced by the net effect of dispersion. This stretched-pulse or dispersion-managed soliton [3], [4] operation exists for net anomalous or small normal GVD and allows femtosecond pulses with up to nanojoule energies and ~10-kW peak power levels. The strong evolution of the pulse within the cavity is a distinct contrast to the static soliton solutions. However, the performance of such a laser can be predicted to some extent by solutions of the Ginzburg–Landau equation with the average parameters of the cavity [5], [6].

Recent work has shown theoretically [7], [8] and experimentally [1], [9] that much higher pulse energies and peak powers can be achieved in fiber lasers that operate at large normal dispersion. In the normal dispersion regime, solitons do not form, so new pulse-shaping processes are needed. The aim of this paper is to present theoretical and intuitive understanding of the pulse-shaping processes and pulse evolutions in normal-dispersion fiber lasers. The results of numerical simulations that accurately model experiments will be presented. Pulses that propagate in normal-dispersion media are susceptible to distortion and breakup owing to optical wave breaking [10]. To compensate nonlinear phase and avoid wave breaking, dissipation is required and plays a key role in the pulse shaping. Several distinct regimes of mode locking can be labeled usefully by the pulse that forms in each one. These include

1. dissipative solitons (DS) [8], [9], [11]–[34];
2. passive similaritons (pulses that evolve in a self-similar fashion have been dubbed similaritons) [35]–[39];
3. amplifier similaritons [40]–[43].

In addition, we consider a pulse evolution that has been exploited experimentally in lasers with dispersion maps but has not been understood theoretically [36], [44]. Ilday *et al.* used the phrase “wave breaking free” to describe these pulses, but that conveys no insight about the pulse formation or evolution that underlies the property. The analysis shows that the pulse formation depends crucially on dissipation, while the evolution is dominated by the presence of the dispersion map. We suggest that these pulses be called stretched dissipative solitons (SDS). These mode-locking regimes will be examined numerically and compared to recent experimental works. For each regime, we will address the following questions.

1. How do the relevant physical processes balance to shape the pulse?
2. What identifies the regime? How is it unique?
3. What are the performance advantages?

This paper is organized as follows. DS in all-normal-dispersion lasers will be explained in Section II. Section III addresses dispersion-managed cavities with net normal GVD. We find that two distinct pulse evolutions can occur for a single set of cavity parameters. The

formation of self-similar pulses in the passive normal-dispersion fiber of a laser (see Section III-A) will be described and contrasted with DS formation. The second regime in a mapped cavity is the SDS. In Section III-B, we show that these pulses are formed similarly to DS, but their evolution is defined by the dispersion map. Section IV considers normal-dispersion lasers in which self-similar evolution occurs in the amplifier, not in passive fiber. Spectral filtering is critical to stabilizing this evolution, which has the remarkable feature of being a local nonlinear attractor in the gain fiber. The different regimes will be summarized and compared in Section V.

II. DS Fiber Lasers

In 2006, Chong *et al.* introduced a new femtosecond mode-locking regime based on cavities with only normal-dispersion components [11]. This was a major departure from prior approaches to femtosecond pulse generation, all of which relied on dispersion compensation. The pulses depend on the balance of both amplitude and phase modulations and are thus considered DS, accurately modeled with a quintic Ginzburg–Landau master equation [8]. To date, the best performance from SMF lasers has been achieved with this mode-locking mechanism. 100-fs pulses with energies of 30 nJ and peak power levels of 300 kW can be generated by lasers based on SMF [9], and megawatt peak power can be reached in large-mode area fiber [29], [32]–[34]. Furthermore, the DS regime has been extended to large net dispersion (> 1 ps^2), which allows for high-energy pulses with large and linear chirp [22]. This giant-chirp oscillator can significantly reduce the complexity of chirped-pulse amplification systems. In this section, the key mechanisms in normal dispersion mode locking will be revealed in the context of an all-normal dispersion DS laser. Specifically, we find that amplitude and phase modulations have equal importance, and that large nonlinear phase shifts are compensated by propagation of a chirped pulse in normal-dispersion fiber. The simulations are designed to model a realistic laser based on Yb:fiber operating at 1 μm. Details and parameters of the simulations are given in the Appendix.

To begin to understand DS mode locking, the fiber sections are modeled as if they are lumped into a single segment of gain fiber, which is the simplest realistic model for a DS fiber laser (see Fig. 1). The resulting pulse parameters and evolution are those of a typical DS laser (see Fig. 2). In the fiber, the spectrum develops structure [see Fig. 2(a)] and the pulse duration increases [see Fig. 2(b)]. The saturable absorber slightly reduces the pulse duration. The spectral filter cuts away the spectral structure and, because the pulse is chirped, restores the pulse to its original duration. Further insight is gained by examining the temporal magnitude and phase. The temporal phase is the same at the end of each segment, which implies that the saturable absorber and the spectral filter have little effect on it. However, if we look into the fiber section [see Fig. 2(c)], we see that the temporal phase evolves in such a way that it begins and ends with the same profile. Thus, for this pulse shape, normal dispersion compensates a self-focusing nonlinear phase shift.

To demonstrate that this picture is not an artifact of combining the fiber sections, and to verify and generalize this conclusion, we also simulate a cavity that artificially separates GVD, nonlinearity, and the saturating gain into independent sections of the oscillator, in that order (see Fig. 3). In this case, as before, the spectrum gains structure in the nonlinear section [see Fig. 4(a)] and the pulse duration increases due to the GVD [see Fig. 4(b)]. The saturable absorber shortens the pulse. Also, as in Fig. 2, the spectral filter cuts away the spectral structure and, because the pulse is chirped, decreases the pulse back to its original duration. The primary difference in this scenario is that the temporal phase evolves in the normal dispersion fiber [see Fig. 4(c)]. However, as in Fig. 2, the change in the phase due to the normal GVD cancels the nonlinear phase shift [see Fig. 4(d)]. The spectral filter also

contributes to the temporal phase, but it is negligible compared to that from the nonlinearity and the normal GVD [see Fig. 4(d)].

Based on the simulations, we can say that linear phase accumulation is balanced by spectral filtering and saturable absorption to create the pulse amplitude, and simultaneously GVD balances the nonlinear phase accumulation in a DS. These balances are illustrated in Fig. 5. Remarkably, a chirped pulse that propagates through normal-GVD material can accumulate a linear phase that is negative, i.e., that one would ordinarily associate with propagation at anomalous GVD. This feature is critical to the generation of high-energy pulses.

III. Dispersion-Managed Fiber Lasers

In a dispersion-managed cavity, several distinct operating regimes exist. Dispersion-managed solitons occur for net GVD near zero, and for large normal GVD, two distinct regimes can coexist for a single set of cavity parameters. One of these regimes features parabolic pulses that evolve self-similarly in a long segment of passive fiber [35]. In section III-A, we will investigate how nonlinearity is managed in this regime, comparing and contrasting with DS mode locking. The second pulse evolution found at large normal GVD was first observed experimentally by Ilday *et al.*, who described it generically as “wave breaking free.” This mode was later exploited by Buckley *et al.* to achieve 100-fs pulses with energy above 10 nJ for the first time. It features highly down-chirped pulses with large breathing ratios and supports stable pulses with peak powers of 100 kW [36], [44]. However, a theoretical understanding has not been reported to date. In section III-B, we will present the first theoretical results that exhibit this evolution. These demonstrate that the pulses are shaped by the same mechanisms as DS, but have additional evolution defined by the particular dispersion map.

We simulate a realistic dispersion-managed cavity as in [36], e.g., (see Appendix B). SMF precedes a Yb-doped gain fiber, which is followed by a saturable absorber, an output coupler and gratings that supply anomalous GVD, in that order (see Fig. 6). We consider only linear anomalous-GVD segments. It is typically desirable to avoid soliton formation in high-energy lasers, which motivates the use of linear anomalous-GVD segments. As a practical matter, in 1-μm systems, the anomalous GVD is commonly provided by diffraction gratings. In most cases, the conclusions we find can be generalized to 1.55-μm systems, where the ready availability of anomalous-dispersion fiber makes nonlinear anomalous-dispersion segments more common. By varying the initial conditions of the simulations slightly (different white noise or Gaussian initial conditions), the two solutions shown in Fig. 7(a) can be seen.

A. Passive Self-Similar Fiber Lasers

The solid line in Fig. 7 is the well-known self-similar pulse solution [35]. The pulses have minimal spectral evolution. They are always positively chirped, with a nearly parabolic pulse profile. The pulse duration increases monotonically in the passive fiber, and the maximum duration occurs at the transition from normal to anomalous dispersion. The temporal breathing ratio ranges from 10 to 50 under typical conditions. The dispersive delay is primarily responsible for returning the pulse to the original duration after a round trip of the cavity. The self-similar pulses can tolerate large nonlinear phase shifts without distortion or wave breaking. As there has been some confusion in the literature, we emphasize that these similaritons are the asymptotic solutions of the nonlinear Schrodinger equation with only nonlinearity and normal GVD. These are distinct from the similaritons that form in the presence of gain, and which constitute nonlinear attractors [45]. The first similariton laser [35] was *not* a similariton amplifier with the cavity feedback.

On initial inspection, it would seem that the self-similar propagation has little relation to DS formation. The initial similariton laser was designed to minimize the effects of gain filtering, which would in turn minimize perturbation of the self-similar propagation. To address these questions, we performed a series of simulations with the parameters varied continuously but with fixed average parameters, and we found that a continuous transition can be made from DS formation to self-similar evolution. (The parameters of the simulations are in Appendix B1.) Thus, we conclude that the self-similar regime does rely on dissipation. It is desirable to have a more detailed understanding of how the temporal amplitude and phase of the pulse balance around the cavity, and this is also provided by the simulations.

The results for the end-points of the series (i.e., the "pure" DS and the passive similariton) are shown in Fig. 8. Although the average parameters of the systems are identical, clear differences remain in the converged solutions. The bandwidth of the DS laser is larger and the spectrum more square [see Fig. 8(a)]. In the DS laser, the increase of the pulse duration from the normal dispersion is compensated by the filter and the saturable absorber, whereas in the mapped cavity, the anomalous dispersion also plays a major role [see Fig. 8(b)]. As expected, the self-similar pulse becomes more parabolic [see Fig. 8(d)] than the DS pulse [see Fig. 8(c)].

To compare the performance of these two systems, the pump power is increased in both the DS and the self-similar cavities with the same net parameters until the maximum energy is reached. As is expected in DS lasers [8], [20], the spectrum of the high energy output becomes broad and structured, and features prominent peaks at the edges (see Fig. 9(a), solid line). The self-similar spectrum, although narrower than the DS spectrum, broadens while it maintains a smooth parabolic profile (see Fig. 9(a), dashed line). Because the bandwidth approaches that of the gain filter, the self-similar pulse has a significant pulse cutting contribution due to the spectral filter (see Fig. 9(b), dashed line). The respective pulse evolutions [see Fig. 9(b)] clearly distinguish the two regimes. Because of the dispersion map, the self-similar pulse is longer and more parabolic [see Fig. 9(d)] than the DS pulse [see Fig. 9(c)].

The numerical solutions confirm the basis of the term self-similar. Fig. 9(f) shows the evolution of the pulse through the fiber section in the self-similar laser. The pulse evolves self-similarly in a parabolic form, while the form of the DS pulse changes continuously and is not self-similar [see Fig. 9(e)]. The maximum output energy for the DS pulse is 30 nJ, and for the self-similar pulse, it is 57 nJ. This difference stems from the extended duration of the self-similar pulse due to the additional dispersion map in the cavity, which decreases the peak power. As another measure of performance, the nonlinear phase $\varphi^{NL} = \int \gamma(z) P_O(z) dz$ is useful for quantifying the peak power that each mechanism can accommodate. $\varphi^{NL} = 10$ for the self-similar mode and $\varphi^{NL} = 20$ for the DS mode. While in this case the energy tolerated by the self-similar mode is greater, it occurs with less total phase shift. This is important because in a real cavity, to operate in the self-similar mode with sufficient pulse breathing, more fiber is necessary, which in turn carries more nonlinearity. As a consequence, the maximum energies for self-similar and DS mode-locking regimes will be comparable.

To illustrate how the basic physical processes balance each other to form a stable self-similar pulse, we examine the evolution of the high-energy self-similar pulse shown in Fig. 9. The spectrum broadens and approaches a parabolic form on propagation in the long passive fiber and is returned to its original form after the gain filter [see Fig. 10(a)]. The temporal profile also broadens as the pulse propagates in the fiber and the positive pulse chirp increases. The anomalous-dispersion segment compensates most of the pulse broadening, with small contributions from the gain filter and the saturable absorber [see Fig.

10(b)]. The large temporal phase accumulation in the fiber is canceled by the dispersive delay [see Fig. 10(c)], with a negligible contribution from the filter [see Fig. 10(d)].

The balancing of amplitude and phase modulations in a self-similar laser are illustrated in Fig. 11. The saturable absorber and the spectral filter play very similar roles as in the DS laser, but the roles of dispersion and nonlinearity play out differently. Of course, the strong evolution in the self-similar laser contrasts with the nearly static solutions in a DS laser. In a self-similar laser, the nonlinearity interacts with the normal dispersion to linearize the spectral phase such that the temporal phase can then be compensated by anomalous dispersion. This can only happen if the pulse shape is near parabolic, as was predicted and demonstrated in [35]. One consequence of this parabolic pulse is its self-similar evolution. This means that attempts to model the self-similar solution must take into account the evolution itself. However, because the amplitude balances are the same as in the DS pulse and because the total GVD balances with the nonlinear phase, we can expect master-equation treatments with average parameters to be useful in modeling self-similar lasers.

B. SDS Fiber Lasers

Perhaps surprisingly, another set of solutions exists in the dispersion-mapped cavity designed to support self-similar pulses in the passive fiber [46]. The solution corresponding to the dashed line in Fig. 7 exhibits the features of the curious regime reported in [36] and [44]. The pulse duration decreases in the normal-dispersion section and increases in the dispersive delay. The evolution in each segment is mostly monotonic as in a self-similar laser, but the variation of the pulse duration is reversed somehow. The pulses depend strongly on dissipative effects such as the gain filter and the saturable absorber. The pulses are predominantly down chirped and can reach the transform limit in the first part of the grating section. Thus, much less dispersion is required to dechirp these pulses outside the cavity than is needed for similaritons. In order to isolate this regime from self-similar propagation, we searched for a parameter that would ensure its existence. We found that the nonlinearity in the first segment of SMF can be varied to determine whether this or the passive self-similar mode exists. We find that this mode will always converge instead of a self-similar pulse in the limit of this nonlinearity becoming small.

We isolate this new regime and exaggerate some of its key features by setting the nonlinearity in the first fiber to zero and by varying the pulse energy (see Appendix B2 for details). Two transform-limited pulse duration minima occur in the evolution. At high energy, the minima occur near each other at the transition from normal to anomalous dispersion. With decreasing energy, the minima shift to the center of the dispersive sections [see Fig. 12(a)]. The spectrum can be cut by the gain filter and grows back in the nonlinear section of fiber after the gain [see Fig. 12(b)]. A crucial point is that the function of the anomalous dispersion and the first section of fiber can be viewed as simply increasing the magnitude of the negative chirp; these sections can be removed and the solution in the gain and the SMF will remain nearly identical, resulting in a DS in an all-normal-dispersion laser [8]. In this simulation, the solution will truly remain identical in the gain because the dispersion in the first SMF and the dispersive delay are equal and opposite. This regime, therefore, is an extension of DS mode-locking toward zero net cavity dispersion because a dispersion map allows for mode-locking at an arbitrary net cavity dispersion. The pulses are DS with an evolution defined by the additional dispersion map. Thus, it seems most informative to refer to these pulses as SDS. Ilday *et al.* had dubbed these pulses “wave breaking free” to refer to a consequence of their evolution, before the evolution itself was understood [44]. This was a generic label, as self-similar pulses and DS also avoid wave breaking at large nonlinear phase shifts. The analysis based on the cubic-quintic Ginzburg-Landau equation of [8] and [20] can be used to understand this regime. For example, higher energy solutions have less chirp and push the point in the gratings where the pulse is

transform limited closer to the output of the laser. Also, as in the all-normal-dispersion case, the spectrum has steep sides and can have peaks on the edges [see Fig. 12(c)]. The SDS regime allows for large pulse energy as is typical for normal dispersion systems; the largest energy shown here is 12 nJ (Fig. 12 solid line). In addition, the pulse duration can be very short (e.g., 45 fs for the 12-nJ case) because of the low values of net GVD possible [21]; hence, the >100-kW peak powers seen in [36]. The temporal breathing in this regime can also be very large; a breathing ratio of ~30 has been observed experimentally and, in the simulated 12-nJ case, the breathing ratio is ~200.

IV. Amplifier-Similariton Fiber Lasers

Recently, a fourth normal dispersion mode-locking mechanism was introduced in which parabolic amplifier similaritons are stabilized in an oscillator [40]–[43]. Spectral filtering is found to be critical to stabilizing the amplifier similaritons in the cavity. The pulse undergoes large (20 times) spectral breathing as it traverses the cavity. Unlike the other three regimes, the amplifier similariton fiber laser relies on a local nonlinear attraction to stabilize the pulse (see Fig. 13). An arbitrary pulse inserted into a gain fiber is nonlinearly attracted to an asymptotically evolving parabolic pulse. The output pulse parameters are entirely determined by the energy of the input pulse and the parameters of the fiber. The challenge is for the pulse to reach this solution in a fiber length compatible with efficient laser design, and filtering can facilitate this. Shorter, nearly transform-limited pulses can reach the amplifier similariton solution in shorter propagation lengths [45]. Oktem *et al.* built a laser in which the parabolic pulse evolves into a soliton in an anomalous dispersion fiber after the gain, which allows for a short transform-limited pulse to return to the input of the gain fiber [40]. Renninger *et al.* showed that a strong spectral filter after the gain fiber can stabilize amplifier similaritons with feedback, so an anomalous-dispersion segment is not needed [41] (see Fig. 14). For fixed chirp, a pulse with a narrower spectrum is shorter and close enough to the transform limit to provide a self-consistent cavity. The resultant pulse after the gain segment is highly parabolic and the spectral profile is distinguished from that in other mode-locking regimes (see Fig. 15). Aguergaray *et al.* built a Raman oscillator with kilometers of gain fiber, which provides enough propagation length for the asymptotic solution to be achieved [42]. Demonstration of stable propagation of amplifier similaritons in three diverse cavities illustrates the robustness of this regime.

The differences between this regime and the others mentioned are related to the fact that the pulse relies on a local attraction in the gain fiber. As a consequence, the behavior and performance of the laser are decoupled from the average cavity parameters. In [41], the pulses are much shorter than would be expected from a master mode-locking model with the average cavity parameters. As a result, the laser should offer flexibility in design for specific performance and future work will address this point experimentally.

V. Discussion of Results

In this section, we will compare and contrast the four operating regimes (see Table I). High-performance short-pulse fiber lasers rely on an exact balance of large accumulated nonlinear phase shifts during one cycle around the cavity. In the normal-dispersion regime, dissipation plays a crucial role in establishing this balance. Dissipative effects such as spectral filtering and saturable absorption enable the stabilization of a chirped pulse in the presence of nonlinearity and normal dispersion. DS, SDS, and passive self-similar lasers rely on this complete balance. Because the effects are important through the traversal of the entire cavity, the average cavity parameters determine the pulse parameters. Master mode-locking models [7], [8] are useful for determining pulse properties for these regimes. Amplifier similariton lasers, however, rely on a local nonlinear attractor and, therefore, will be less

amenable to such analyses. This opens up interesting possibilities that may go against conventional laser wisdom, such as operation at net zero dispersion or ultrashort pulse durations at large normal dispersion.

The SDS and passive self-similar regime require dispersion-managed cavities. From a physical perspective, this means that the mode-locking mechanism is more complicated, as the evolution of the pulse is important. As an example, mathematically these two regimes are bistable in the same cavity, which leads to a wealth of interesting nonlinear dynamical behavior. From a practical perspective, a dispersion-managed cavity allows for a precise tunability of the net dispersion at the cost of some complexity and loss in the design. However, tuning the net dispersion can allow the generation of DS with shorter duration than can be reached in all-normal-dispersion cavities.

Dispersion managed solitons can also exist in a dispersion managed cavity. In fact, the temporal evolution of these pulses resembles that in Fig. 12(a) (dotted line), but the mode-locking mechanism is distinctly different. Dispersion-managed solitons exist from net anomalous dispersion to slightly normal dispersion when there are minimal dissipative perturbations. In the normal dispersion regime, particularly near zero dispersion, dissipative effects such as gain filtering play a major role. There is extensive literature on dispersion-managed solitons, so we have restricted our discussion to high-energy mode-locking regimes, which exploit (and in fact depend on) dissipative mechanisms.

In the initial development of DS lasers, the acronym ANDi fiber laser, for all-normal dispersion fiber laser, was used. This name was given in reference to the design of the system more than to the pulse-shaping mechanisms. Because amplifier similariton fiber lasers can also exist in an all-normal dispersion cavity, we refer instead to the relevant physical mechanisms: DS mode locking or amplifier similariton mode locking.

Both active and passive self-similar pulses have been stabilized in fiber lasers. In the passive case, this coincides with temporal breathing, which leads to longer durations and large pulse energy. In addition, a parabolic pulse and spectrum can be attractive for applications owing to good pulse quality. In the active case, the nonlinear attraction of the gain fiber is responsible for the mode locking of the laser. In this case, dissipation plays a supporting role by facilitating creation of a self-consistent cavity.

Pulse quality is a critical feature for applications of mode-locked lasers. With proper design, the pulses from almost all of the regimes can be compressed to within 5% of the transform limit. The exception is the giant-chirp oscillator [22]. This is a property of the solution of the equation that models the cavity with very large GVD. Pulses from a giant-chirp oscillator can be dechirped to ~2 times the transform-limit. Another issue that affects pulse quality is the spectral shape of the output of most normal-dispersion lasers. The square, or steep-sided, spectral shape has a sinc function Fourier transform. As a consequence, the transform-limited pulses have low-intensity wings in their temporal profile. These typically contain ~5% of the pulse energy. The exception is the amplifier similariton regime, where the spectra approach a parabolic form that yields dechirped pulses with less energy in the wings.

For many applications, the square or peaked spectral shapes produced by normal-dispersion lasers will be perfectly acceptable. This is the case in nonlinear microscopy, e.g., where the peak power is the most important parameter. However, a smoother spectral shape may be needed for other applications. In this case, a smoother spectrum can be obtained by taking the output after the filter. The structured spectra of normal-dispersion lasers would appear to be a concern for subsequent amplification. In chirped-pulse amplification, spectral modulations can grow as nonlinear phase is accumulated. Ilday *et al.* have shown that the spectral structure can be smoothed by the amplification process [47]. Finally, nonlinear and

dispersive propagation of pulses from normal-dispersion lasers is quantitatively different from the propagation of Gaussian pulses. One must account for this is the design of a pulse compressor, for example.

For the shortest pulses, for the mode-locking mechanisms where the average cavity parameters are important, the laser must be operated as close as possible to net zero dispersion. Consequently, the passive self-similar and SDS regimes are preferable. For short-pulse operation in the amplifier similariton laser, the bandwidth is only limited by the gain bandwidth. Initial demonstrations already include promising results (~55 fs). For energy, however, little is known about the preferred operation regime. To date, DS mode locking achieves the highest performances with >100-nJ pulse energies.

VI. Conclusion

A numerical investigation into fiber lasers mode-locked with net normal dispersion reveals several distinct regimes, including active and passive similariton mode locking, along with dissipative and SDS mode locking. Each regime balances the linear and nonlinear phase accumulations as well as the amplitude modulations. Wave breaking is avoided with a unique combination of normal dispersion and dissipation in each regime. A DS is a chirped pulse that can balance nonlinear phases by spectral filtering and saturable absorption. An SDS provides the same balance but with additional temporal evolution defined by a linear dispersion map. Remarkably, a passive similariton solution can exist in an SDS cavity, but with a very different evolution. In this regime, the spectral filer and saturable absorber still play important roles in creating the pulse, but anomalous dispersion also becomes important. A parabolic pulse evolving self-similarly linearizes the nonlinear phase in the normal dispersion fiber, which is compensated by a dispersion delay. Because of the clear similarities to DS mode locking, master equation models can be used to model passive similariton lasers but, for a complete understanding, the evolution must also be taken into account. Finally, the amplifier similariton regime is distinguished from the other three regimes because it relies on local nonlinear attraction in the gain fiber of the laser. As a consequence, the behavior and performance is decoupled from the average cavity parameters, and this will allow flexibility in design for specific performance.

Acknowledgments

The authors would like to thank Y. Deng and J. Kafka for stimulating discussions.

This work was supported in part by the National Science Foundation under Grant ECS-0500956 and Grant PHY-0653482 and in part by the National Institutes of Health under Grant EB002019.

References

1. Wise FW, Chong A, Renninger WH. High-energy femtosecond fiber lasers based on pulse propagation at normal dispersion. Laser Photon Rev. 2008; 2:58–73.
2. Haus HA, Ippen EP, Tamura K. Additive-pulse modelocking in fiber lasers. IEEE J Quantum Electron. Jan; 1994 30(1):200–208.
3. Tamura K, Ippen E, Haus H, Nelson L. 77-fs pulse generation from a stretched-pulse mode-locked all-fiber ring laser. Opt Lett. 1993; 18:1080–1082. [PubMed: 19823296]
4. Ober MH, Hofer M, Fermann ME. 42-fs pulse generation from a mode-locked fiber laser started with a moving mirror. Opt Lett. 1993; 18:367–369. [PubMed: 19802138]
5. Haus HA, Tamura K, Nelson LE, Ippen EP. Stretched-pulse additive pulse mode-locking in fiber ring lasers: Theory and experiment. IEEE J Quantum Electron. Mar; 1995 31(3):591–598.
6. Malomed, BA. Soliton Management in Periodic Systems. New York: Springer Science+Business Media; 2006.

7. Haus HA, Fujimoto JG, Ippen EP. Structures for additive pulse mode locking. J Opt Soc Amer B. 1991; 8:2068–2076.
8. Renninger WH, Chong A, Wise FW. Dissipative solitons in normal-dispersion fiber lasers. Phys Rev A. 2008; 77:023814-1–023814-4.
9. Kieu K, Renninger WH, Chong A, Wise FW. Sub-100 fs pulses at watt-level powers from a dissipative-soliton fiber laser. Opt Lett. 2009; 34:593–595. [PubMed: 19252562]
10. Anderson D, Desaix M, Lisak M, Quiroga-Teixeiro ML. Wave breaking in nonlinear-optical fibers. J Opt Soc Amer B. 1992; 9:1358–1361.
11. Chong A, Buckley J, Renninger W, Wise F. All-normal-dispersion femtosecond fiber laser. Opt Exp. 2006; 14:10095–10100.
12. Zhao LM, Tang DY, Wu J. Gain-guided soliton in a positive group-dispersion fiber laser. Opt Lett. 2006; 31:1788–1790. [PubMed: 16729071]
13. Soto-Crespo JM, Akhmediev NN, Afanasjev VV, Wabnitz S. Pulse solutions of the cubic-quintic complex Ginzburg–Landau equation in the case of normal dispersion. Phys Rev E. 1997; 55:4783–4796.
14. Lou JW, Currie M, Fatemi FK. Experimental measurements of solitary pulse characteristics from an all-normal-dispersion Yb-doped fiber laser. Opt Exp. 2007; 15:4960–4965.
15. Prochnow O, Ruehl A, Schultz M, Wandt D, Kracht D. All-fiber similariton laser at 1 μm without dispersion compensation. Opt Exp. 2007; 15:6889–6893.
16. An J, Kim D, Dawson JW, Messerly MJ, Barty CPJ. Grating-less, fiber-based oscillator that generates 25 nJ pulses at 80 MHz, compressible to 150 fs. Opt Lett. 2007; 32:2010–2012. [PubMed: 17632626]
17. Chong A, Renninger WH, Wise FW. All-normal-dispersion femtosecond fiber laser with pulse energy above 20 nJ. Opt Lett. 2007; 32:2408–2410. [PubMed: 17700801]
18. Ortaç B, Schmidt O, Schreiber T, Limpert J, Tünnermann A, Hideur A. High-energy femtosecond Yb-doped dispersion compensation free fiber laser. Opt Exp. 2007; 15:10725–10732.
19. Ortaç B, Plötner M, Limpert J, Tünnermann A. Self-starting passively mode-locked chirped-pulse fiber laser. Opt Exp. 2007; 15:16794–16799.
20. Chong A, Renninger WH, Wise FW. Properties of normal-dispersion femtosecond fiber lasers. J Opt Soc Amer B. 2008; 25:140–148.
21. Chong A, Renninger WH, Wise FW. Route to the minimum pulse duration in normal-dispersion fiber lasers. Opt Lett. 2008; 33:2638–2640. [PubMed: 19015693]
22. Renninger WH, Chong A, Wise F. Giant-chirp oscillators for short-pulse fiber amplifiers. Opt Lett. 2008; 33:3025–3027. [PubMed: 19079529]
23. Bale BG, Kutz JN, Chong A, Renninger WH, Wise FW. Spectral filtering for mode locking in the normal dispersive regime. Opt Lett. 2008; 33:941–943. [PubMed: 18451946]
24. Chong A, Renninger WH, Wise FW. Environmentally stable all-normal-dispersion femtosecond fiber laser. Opt Lett. 2008; 33:1071–1073. [PubMed: 18483515]
25. Kieu K, Wise FW. All-fiber normal-dispersion femtosecond laser. Opt Exp. 2008; 33:11453–11458.
26. Bale BG, Kutz JN, Chong A, Renninger WH, Wise FW. Spectral filtering for high-energy mode-locking in normal dispersion fiber lasers. J Opt Soc Amer B. 2008; 25:1763–1770.
27. Schultz M, Karow H, Prochnow O, Wandt D, Morgner U, Kracht D. All-fiber ytterbium femtosecond laser without dispersion compensation. Opt Exp. 2008; 16:19562–19567.
28. Akhmediev N, Soto-Crespo JM, Grelu P. Roadmap to ultra-short record high-energy pulses out of laser oscillators. Phys Lett A. 2008; 372:3124–3128.
29. Ortaç B, Baumgartl M, Limpert J, Tünnermann A. Approaching microjoule-level pulse energy with mode-locked femtosecond fiber lasers. Opt Lett. 2009; 34:1585–1587. [PubMed: 19448829]
30. Renninger WH, Chong A, Wise FW. Area theorem and energy quantization for dissipative optical solitons. J Opt Soc Amer B. 2010; 27:1978–1982. [PubMed: 21765589]
31. Özgören K, Ilday FÖ. All-fiber all-normal dispersion laser with a fiber-based Lyot filter. Opt Lett. 2010; 35:1296–1298. [PubMed: 20410998]

32. Lefrancois S, Kieu K, Deng Y, Kafka JD, Wise FW. Scaling of dissipative soliton fiber lasers to megawatt peak powers by use of large-area photonic crystal fiber. Opt Lett. 2010; 35:1569–1571. [PubMed: 20479811]
33. Baumgartl M, Ortaç B, Lecaplain C, Hideur A, Limpert J, Tünnermann A. Sub-80 fs dissipative soliton large-mode-area fiber laser. Opt Lett. 2010; 35:2311–2313. [PubMed: 20596230]
34. Lecaplain C, Ortaç B, Machinet G, Boullet J, Baumgartl M, Schreiber T, Cormier E, Hideur A. High-energy femtosecond photonic crystal fiber laser. Opt Lett. 2010; 35:3156–3158. [PubMed: 20890318]
35. Ilday FÖ, Buckley JR, Clark WG, Wise FW. Self-similar evolution of parabolic pulses in a laser. Phys Rev Lett. 2004; 92:213902-1–213902-4. [PubMed: 15245282]
36. Buckley J, Wise F, Ilday F, Sosnowski T. Femtosecond fiber lasers with pulse energies above 10 nJ. Opt Lett. 2005; 30:1888–1890. [PubMed: 16092379]
37. Nielsen C, Ortaç B, Schreiber T, Limpert J, Hohmuth R, Richter W, Tünnermann A. Self-starting self-similar all-polarization maintaining Yb-doped fiber laser. Opt Exp. 2005; 13:9346–9351.
38. Ruehl A, Prochnow O, Wandt D, Kracht D, Burgoyne B, Godbout N, Lacroix S. Dynamics of parabolic pulses in an ultrafast fiber laser. Opt Lett. 2006; 31:2734–2736. [PubMed: 16936874]
39. Ortaç B, Hideur A, Chedot C, Brunel M, Martel G, Limpert J. Self-similar low-noise femtosecond ytterbium-doped double-clad fiber laser. Appl Phys B. 2006; 85:63–67.
40. Oktem B, Ulgudur FO, Ilday FO. Soliton-similariton fibre laser. Nature Photon. 2010; 4:307–311.
41. Renninger WH, Chong A, Wise F. Self-similar pulse evolution in an all-normal-dispersion laser. Phys Rev A. 2010; 82:021805-1–021805-4. [PubMed: 21765623]
42. Aguergaray C, Méchin D, Kruglov V, Harvey JD. Experimental realization of a Mode-locked parabolic Raman fiber oscillator. Opt Exp. 2010; 18:8680–8687.
43. Bale BG, Wabnitz S. Strong spectral filtering for a mode-locked similariton fiber laser. Opt Lett. 2010; 35:2466–2468. [PubMed: 20634865]
44. Ilday FÖ, Buckley J, Lim H, Wise F, Clark W. Generation of 50-fs, 5-nJ pulses at 1.03 μm from a wave-breaking-free fiber laser. Opt Lett. 2003; 28:1365–1367. [PubMed: 12906091]
45. Fermann ME, Kruglov VI, Thomsen BC, Dudley JM, Harvey JD. Self-similar propagation and amplification of parabolic pulses in optical fibers. Phys Rev Lett. 2000; 84:6010–6013. [PubMed: 10991111]
46. Schreiber T, Ortaç B, Limpert J, Tünnermann A. On the study of pulse evolution in ultra-short pulse mode-locked fiber lasers by numerical simulations. Opt Exp. 2007; 15:8252–8262.
47. Mukhopadhyay PK, Özgören K, Budunoglu IL, Ilday FÖ. All-fiber low-noise high-power femtosecond Yb-fiber amplifier system seeded by an all-normal dispersion fiber oscillator. IEEE J Sel Topics Quantum Electron. Jan-Feb;2009 15(1):145–152.

Biographies

William H. Renninger received the B.S. degree in applied physics from Cornell University, Ithaca, NY, in 2006, where he is currently working toward the Ph.D. degree in applied physics.

His research interests include nonlinear optics and ultrafast phenomena.

Andy Chong received the B.S. degrees in mechanical engineering and physics from the University of Texas at Austin, Austin, in 1996. After working for several companies, he received the Ph.D. degree in applied physics from Cornell University, Ithaca, NY, in 2008.

He is currently a Postdoctoral Researcher at Cornell University in nonlinear optics and ultrafast pulse propagation phenomena.

Frank W. Wise received the B.S. degree from Princeton University, Princeton, NJ, the M.S. degree from the University of California, Berkeley, and the Ph.D. degree from Cornell University, Ithaca, NY.

Since receiving the Ph.D. degree in 1988, he has been at the Faculty in the Department of Applied Physics at Cornell University.

Appendix: Simulation Parameters

A. DS Cavity

Simulations are solved with a standard symmetric split-step propagation algorithm. Passive SMFs are modeled with the nonlinear Schrodinger equation with $\beta_2 = 230$ fs^2/cm and $\gamma = 0.0047$ (W m)$^{-1}$. The active fiber is modeled by a saturating gain, $g = g_o/(1 + E_{\text{pulse}}/E_{\text{sat}})$, where g_o corresponds to 30 dB of small-signal gain, $E_{\text{pulse}} = \int_{-T_R/2}^{T_R/2} |A|^2 dt$, where A is the electric field envelope, τ_R is the cavity round trip time, and E_{sat} is the gain saturation energy. The fiber is followed by a saturable absorber given by a monotonically increasing transfer function, $T = 1 - l_o/[1 + P(\tau)/P_{\text{sat}}]$ where l_o is the unsaturated loss, $P(\tau)$ is the instantaneous pulse power, and P_{sat} is the saturation power. The absorber is followed by a variable output coupler. The cavity consists of a single 6-m segment of gain fiber with $E_{\text{sat}} = 7.2$ nJ. After the fiber is a saturable absorber with $l_o = 0.7$ and $P_{\text{sat}} = 3$ kW, a spectral filter with 12-nm bandwidth, and an 88% output coupler. The simulation is seeded with a picosecond Gaussian temporal profile and run until the pulse energy converges; the resultant output pulse energy is 12 nJ.

B. Dispersion-Managed Cavity

A 450-cm segment of SMF precedes 25 cm of highly Yb-doped gain fiber, and a 20-cm segment follows it. The gain fiber includes a 40-nm distributed Gaussian filter and no

additional spectral filter is included. After the fiber section are the diffraction gratings, modeled as an anomalous dispersive delay, the dispersion of which is varied to achieve a particular net GVD. The cavity has a net dispersion of 5000 fs^2 , $I_o = 0.7$, 90% output coupling, 80% additional loss from the gratings and the collimator, $P_{sat} = 5$ kW, and $E_{sat} = 1.2$ nJ.

1) Passive Self-Similar Mode Locking

The cavity consists of 25 cm of SMF with varying normal GVD, a section with saturating gain and a gain filter with 40-nm bandwidth, a saturable absorber with $I_o = 0.7$, a 70% output coupler, and a section with variable anomalous GVD. If the anomalous GVD section is absent, the cavity represents a DS with 5000 fs^2 net dispersion. If the magnitude of anomalous dispersion is increased and an equal amount of normal dispersion is added to the fiber section, the net cavity dispersion will remain at 5000 fs^2 but the dispersion map will increase, modeling the cavity of a self-similar laser. The dispersion map was increased until the simulations no longer converged, with a dispersion of −110 000 fs^2 in the anomalous dispersion segment.

2) SDS Mode Locking

Simulations are run with the net GVD = 5000 fs^2 , $I_o = 0.7$, 90% output coupling, 50% additional loss from the gratings and the collimator, no nonlinearity in the first fiber, $P_{sat} =$ 1, 6, and 21 kW, and $E_{sat} = 0.2$, 1.4, and 5.0 nJ.

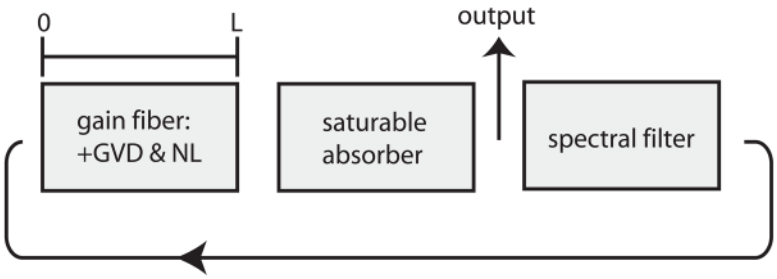

Fig. 1.
Schematic of the simplest all-normal dispersion DS laser.

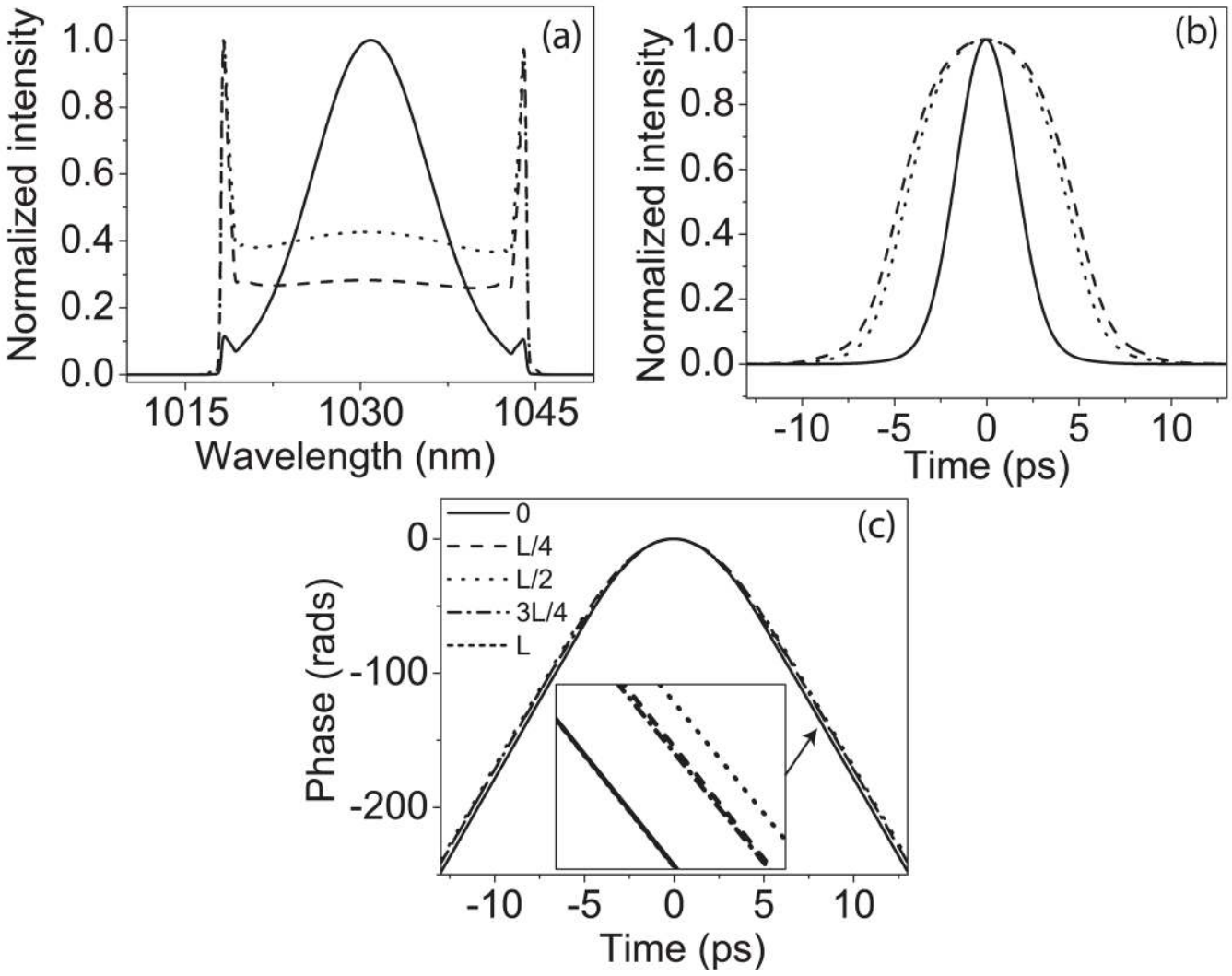

Fig. 2.

Evolution of the (a) spectrum and (b) temporal profile of a DS plotted after the filter (solid), after the fiber (dashed), and after the saturable absorber (dotted). (d) Evolution of the temporal phase in the fiber section.

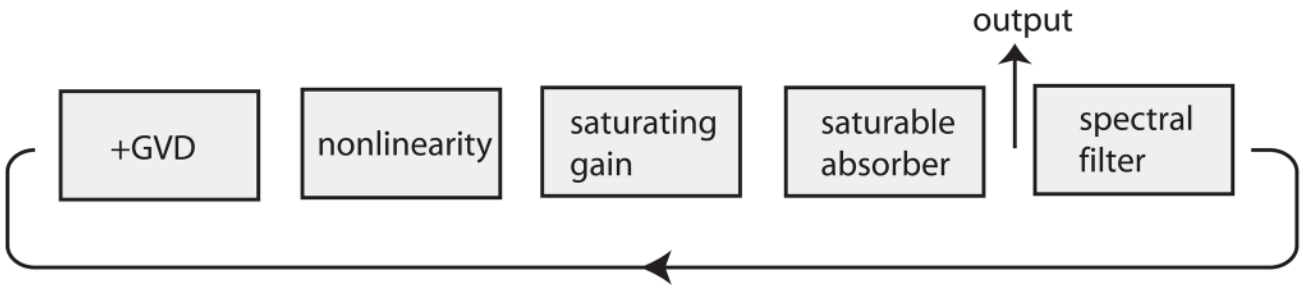

Fig. 3.
Schematic of an all-normal dispersion DS laser with physical processes separated for clarity.

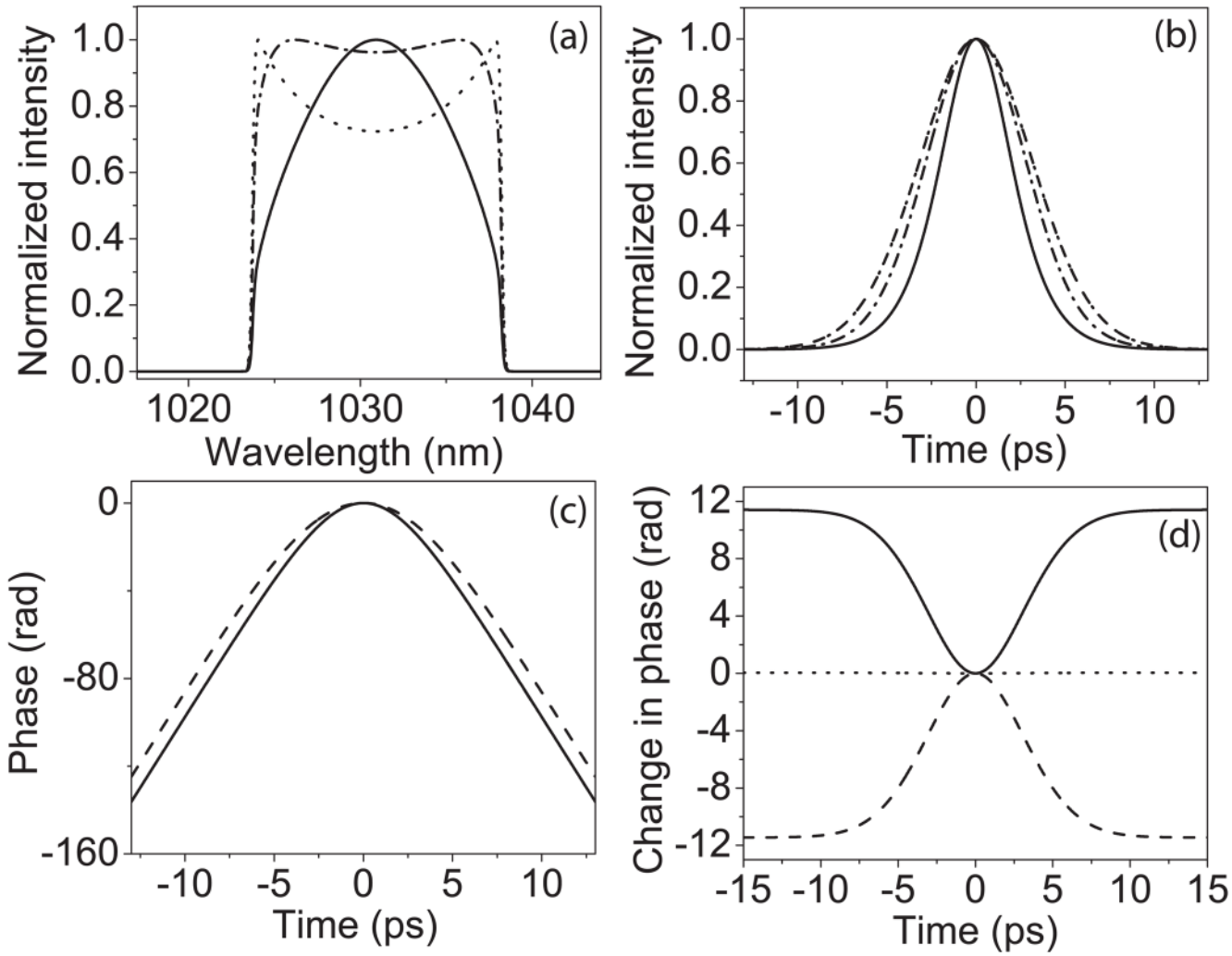

Fig. 4.

Evolution of the (a) spectrum, (b) pulse, and (c) temporal phase of the solution to a normal dispersion oscillator plotted after the filter (solid), after the GVD (dashed), after the nonlinearity (dotted), and after the saturable absorber (dashed-dotted). (d) Change in phase due to the GVD (solid), nonlinearity (dashed), and spectral filter (dotted).

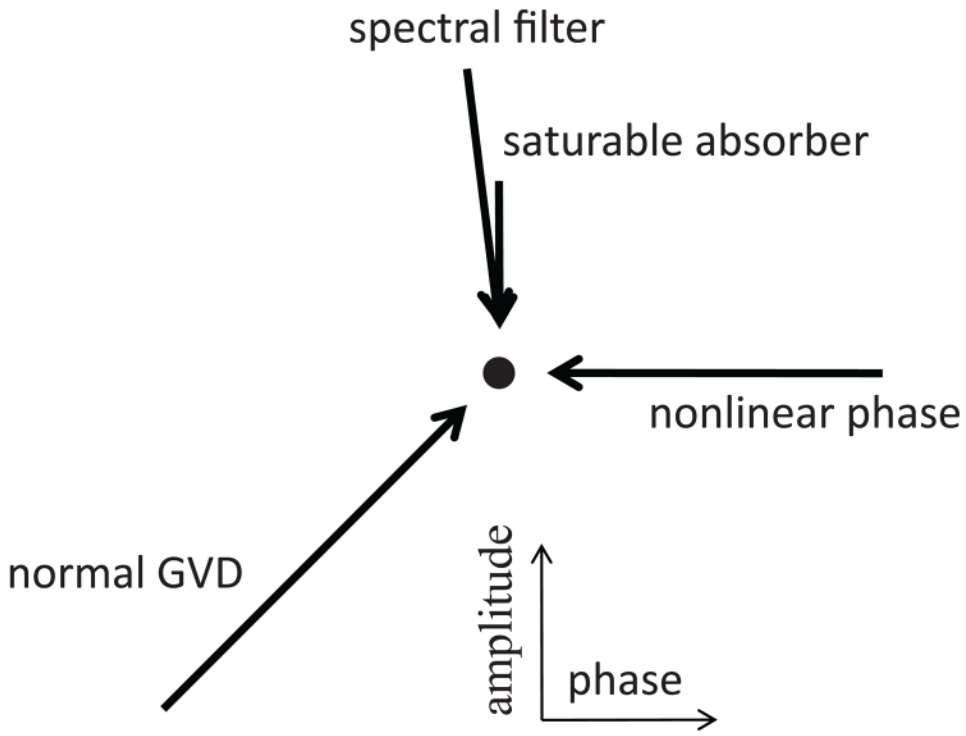

Fig. 5.
Qualitative illustration of the amplitude and phase balances in a DS laser.

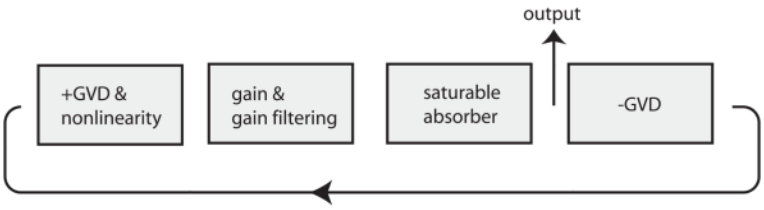

Fig. 6.
Schematic of a typical 1-μm dispersion-managed fiber laser.

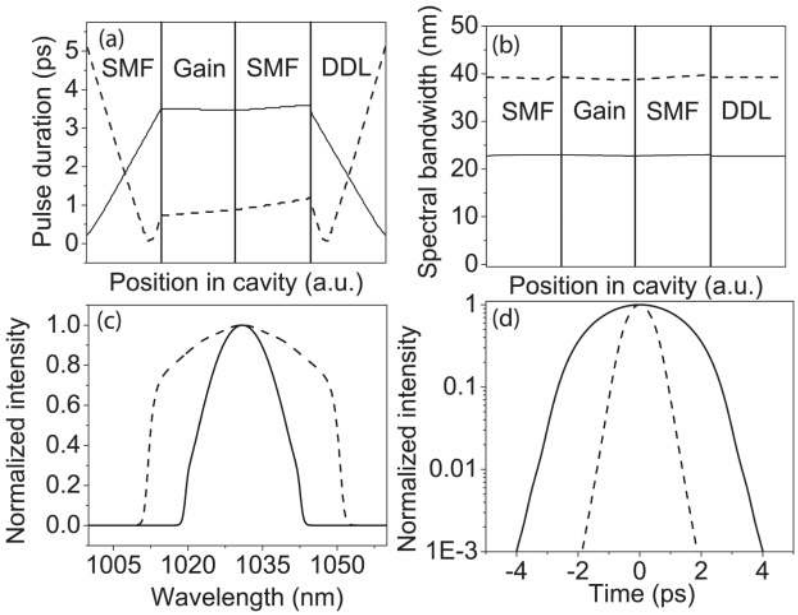

Fig. 7.

Evolution of the (a) pulse duration (the full-width at half of the maximum) and (b) spectral bandwidth (the full-width at a fifth of the maximum) and output (c) spectra and (d) chirped pulses for self-similar (solid) and SDS (dashed) mode-locked pulses given identical cavity parameters. DDL: dispersive delay line.

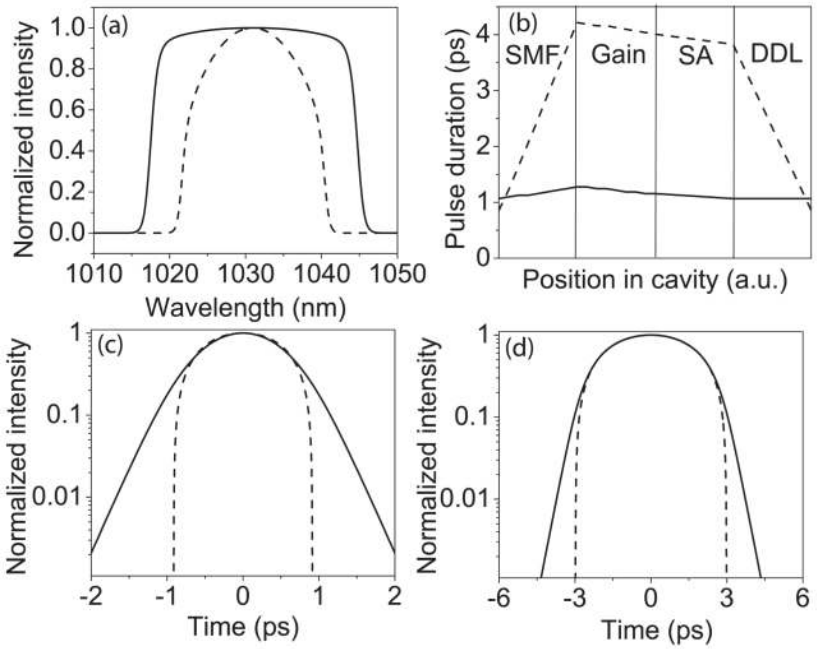

Fig. 8.

(a) Spectrum after the first SMF and (b) temporal evolution of the DS (solid) and self-similar (dashed) pulses. (c) Pulse after the first SMF for the DS and the (d) self-similar pulses; the dotted lines represent parabolic fits.

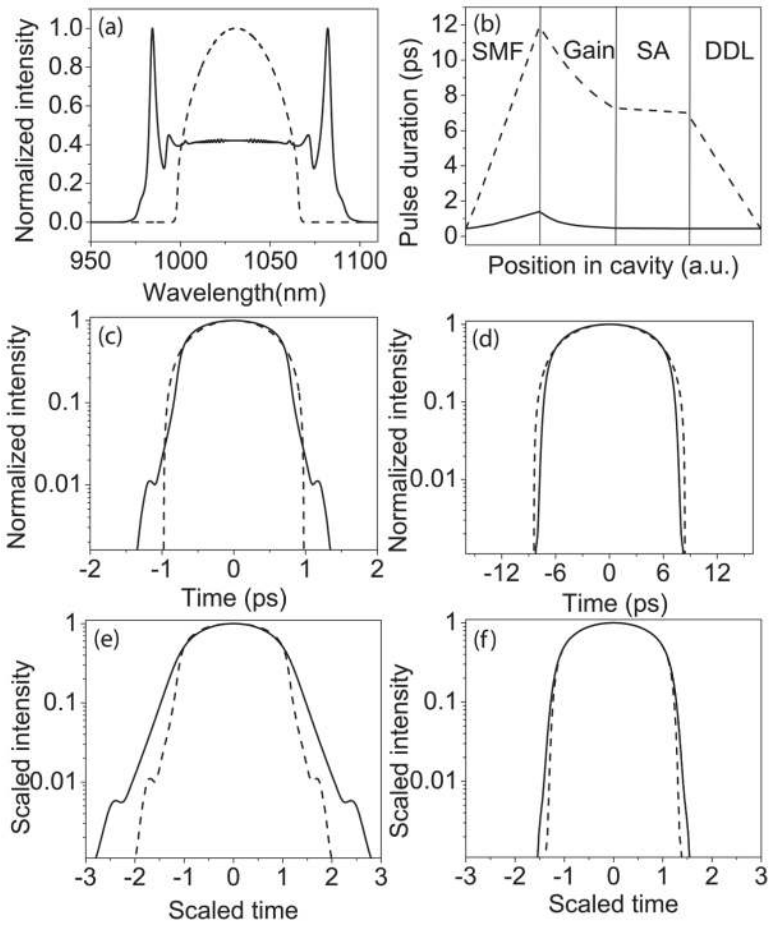

Fig. 9.

(a) Spectrum after the first SMF and (b) temporal evolution of the DS (solid) and self-similar (dashed) pulses. Pulse after the first SMF for the (c) DS and the (d) self-similar pulses; the dashed lines represent parabolic fits. Temporal evolution of the pulse in the first section of the fiber of the (e) DS laser and the (f) self-similar laser; the dashed (solid) line represents propagation through half (all) of the fiber.

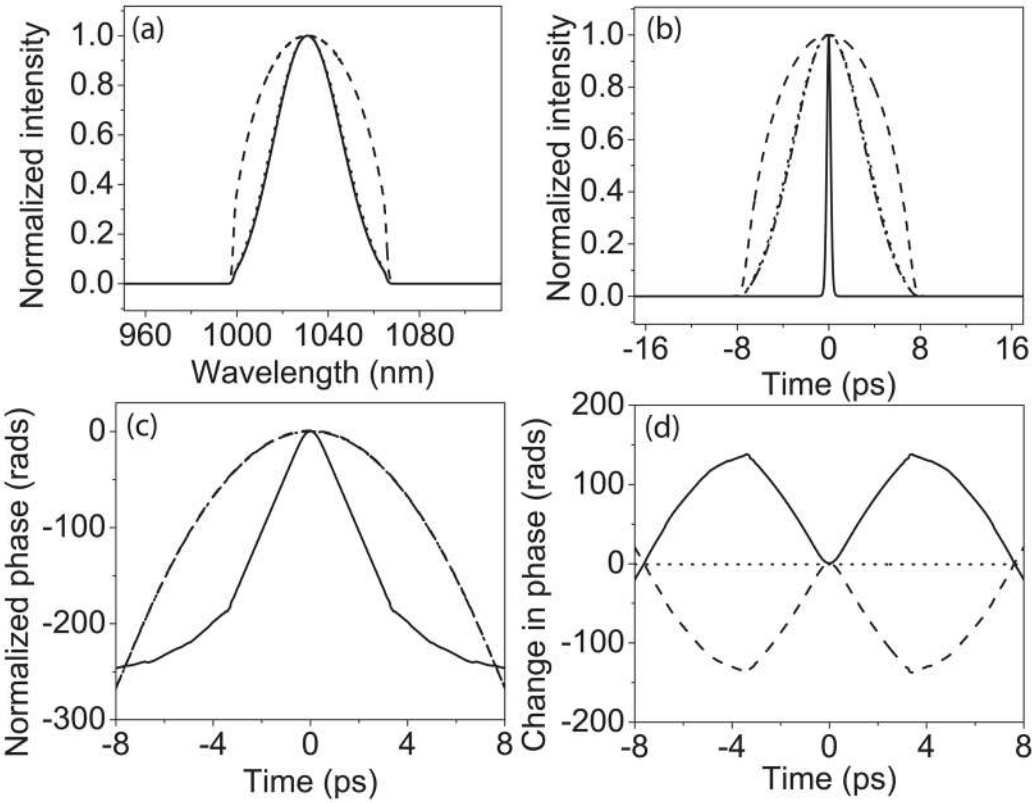

Fig. 10.

Evolution of the (a) spectrum, (b) pulse, and (c) temporal phase of the solution to a normal dispersion oscillator plotted after the filter (solid), after the GVD (dashed), after the nonlinearity (dotted), and after the saturable absorber (dashed-dotted). (d) Change in phase due to the SMF (dashed), anomalous GVD (dashed), and spectral filter (dotted).

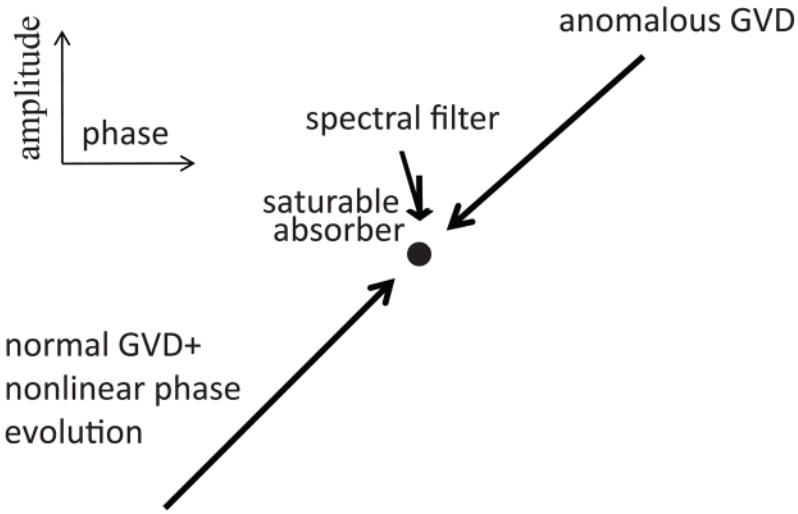

Fig. 11.
Qualitative illustration of the amplitude and phase balances in a passive self-similar laser.

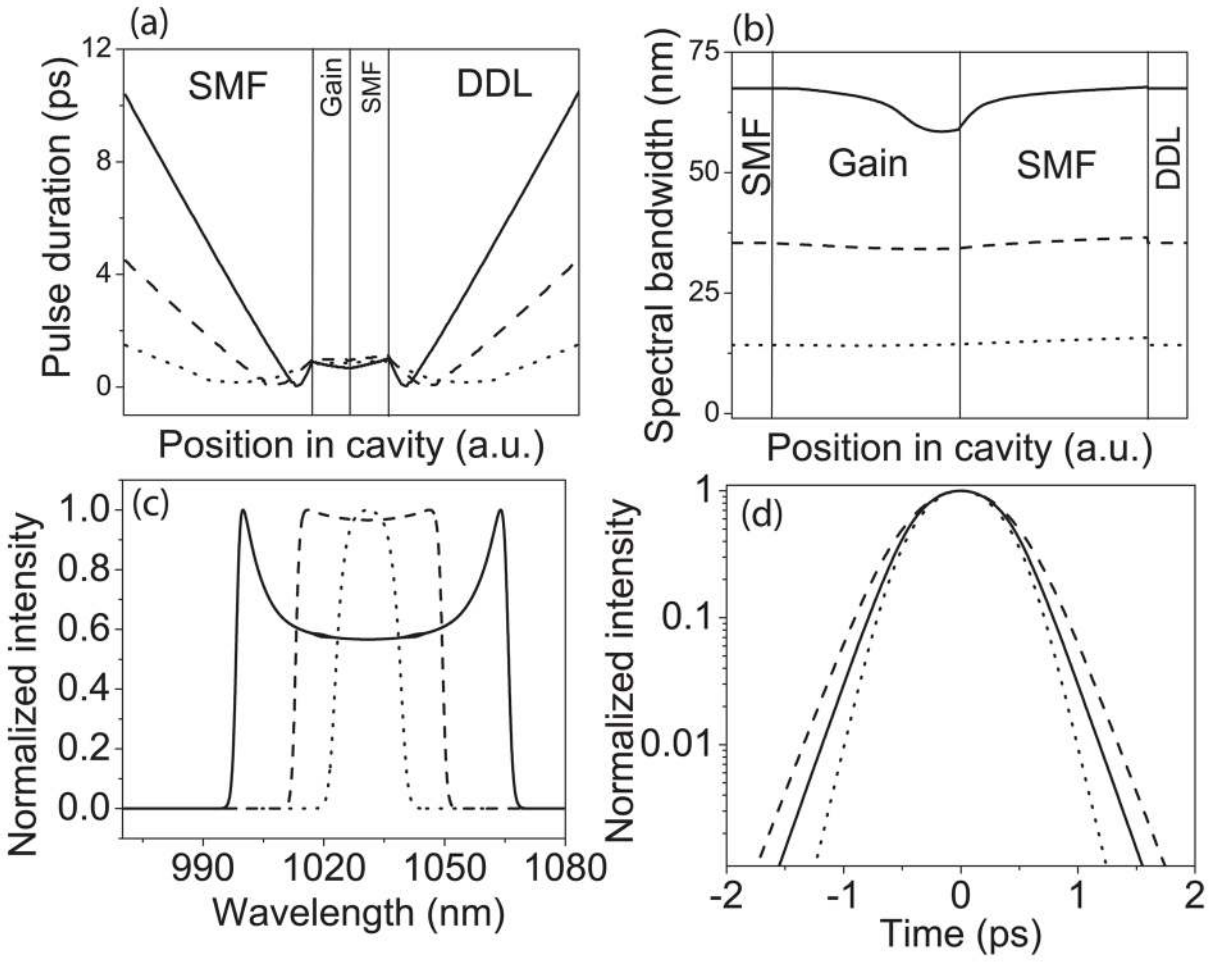

Fig. 12.

Evolution of (a) pulse duration and (b) spectral bandwidth, and output (c) spectra and (d) pulses of an SDS laser for 1 nJ (dotted line), 4 nJ (dashed line), and 12 nJ (solid line) intracavity pulse energies.

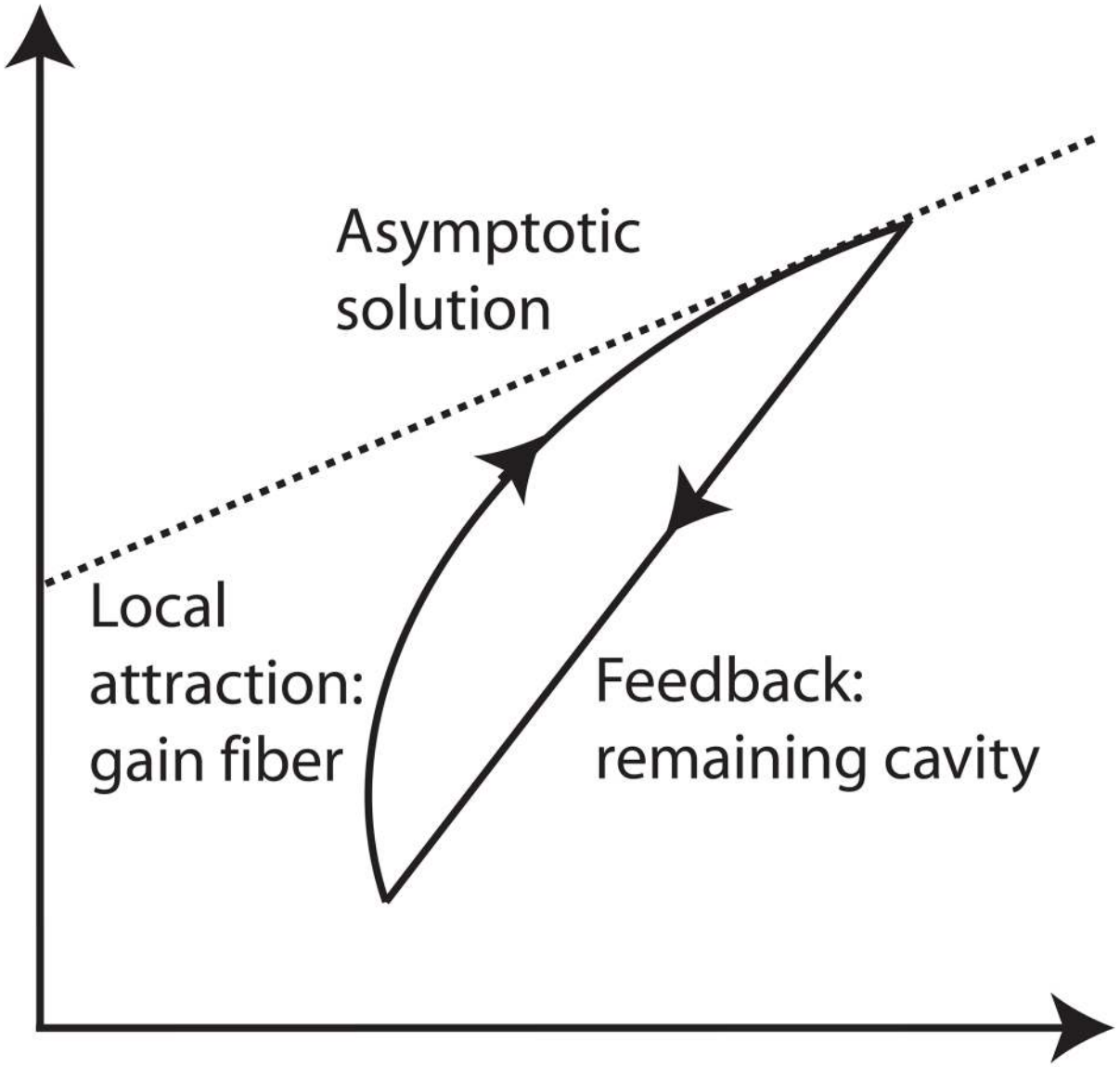

Fig. 13.
Illustration of the local attraction in an amplifier similariton fiber laser. The inset shows the output pulse (solid) and parabolic fit (dotted) from the numerical results in [41], representing the asymptotic solution.

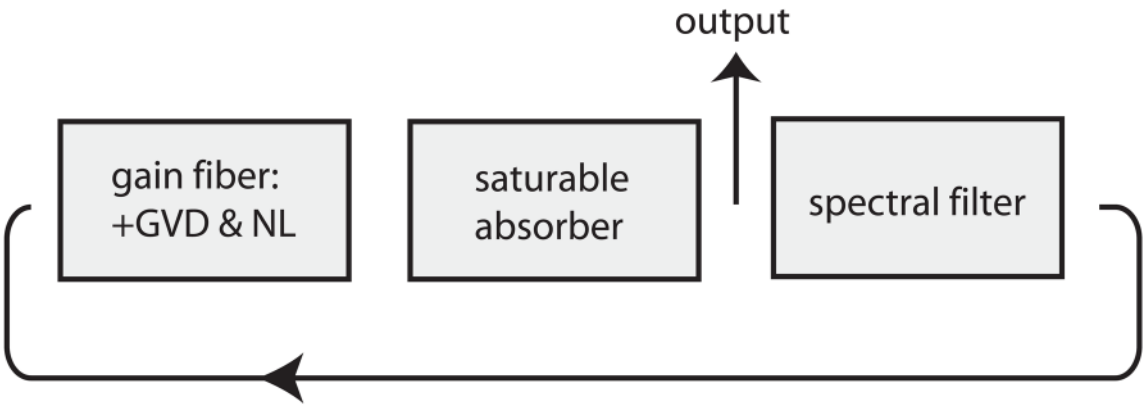

Fig. 14.
Cartoon schematic of an amplifier similariton fiber laser.

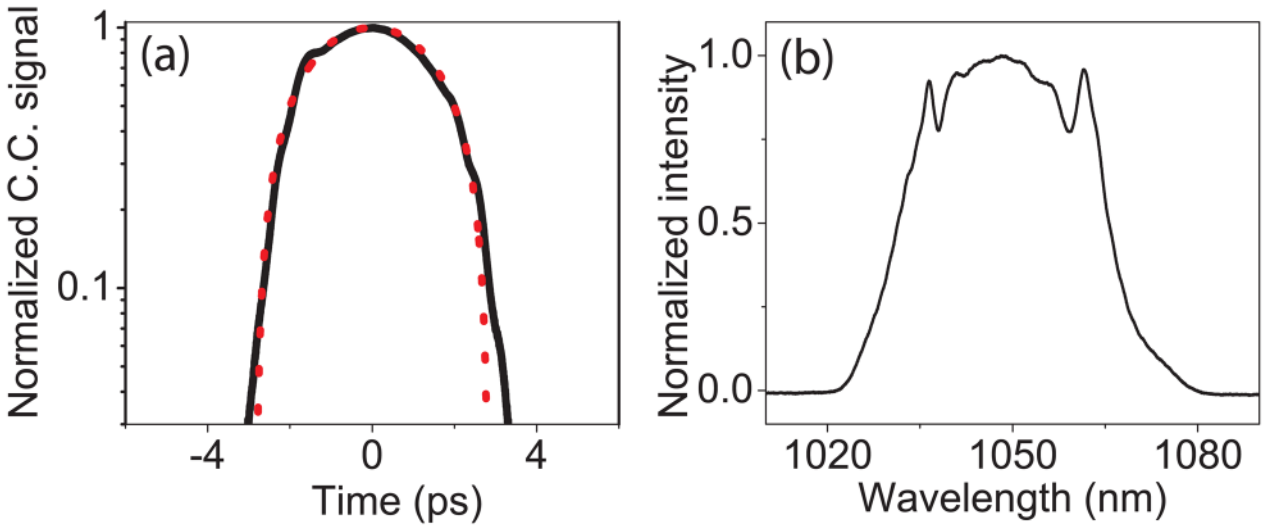

Fig. 15.
(a) Cross correlation (C.C.) of the pulse (with dotted parabolic fit). (b) Spectrum after propagation through the gain fiber.

TABLE 1

Comparison of Important Features

	DS	SDS	Passive SS	Active SS
Average cavity parameters	✓	✓	✓	
Dispersion map		✓	✓	
Self-similar/parabolic			✓	✓

Note: DS: dissipative soliton, SDS: stretched dissipative soliton, SS: self-similar.